

Article

# Experimental Study on NO<sub>x</sub> Reduction in Oxy-fuel Combustion Using Synthetic Coals with Pyridinic or Pyrrolic Nitrogen

Chang'an Wang, Pengqian Wang, Lin Zhao, Yongbo Du and Defu Che \*

State Key Laboratory of Multiphase Flow in Power Engineering, School of Energy and Power Engineering, Xi'an Jiaotong University, Xi'an 710049, China; changanwang@mail.xjtu.edu.cn (C.W.); xjppqwang@stu.xjtu.edu.cn (P.W.); 13709122991@163.com (L.Z.); ybdu\_boilerynwa@mail.xjtu.edu.cn (Y.D.)

\* Correspondence: dfche@mail.xjtu.edu.cn; Tel.: +86-029-82668703

Received: 11 November 2018; Accepted: 3 December 2018; Published: 5 December 2018



**Abstract:** Oxy-fuel combustion technology can capture carbon dioxide (CO<sub>2</sub>) in the large-scale and greatly lower nitrogen oxides (NO<sub>x</sub>) emission in coal-fired power plants. However, the influence of inherent minerals on NO<sub>x</sub> reduction still remains unclear and the impact of oxy-fuel combustion on the transformation of different nitrogen functional groups has yet to be fully understood. The present work aims to obtain a further understanding of the NO<sub>x</sub> reduction during oxy-fuel combustion using synthetic coals with pyrrolic or pyridinic nitrogen. Compared to pyridinic nitrogen, more of the pyrrolic nitrogen in synthetic coal was converted to NO<sub>x</sub>. The conversion ratio of nitric oxide (NO) first increased significantly with the rising oxygen content and then trended to an asymptotically constant as the oxygen (O<sub>2</sub>) content varied between 10–50%. The nitrogen dioxide (NO<sub>2</sub>) formation was roughly proportional to the oxygen content. The NO<sub>2</sub> conversion was increased with particle size but the case of NO showed a non-monotonic variation. The catalytic effects of sodium carbonate (Na<sub>2</sub>CO<sub>3</sub>), calcium carbonate (CaCO<sub>3</sub>), and ferric oxide (Fe<sub>2</sub>O<sub>3</sub>) on the transformation of pyridinic nitrogen to NO were independent of the combustion atmosphere, while the alteration from air to the oxy-fuel combustion led to a change of mineral catalytic effect on the oxidation of pyrrolic nitrogen within the coal matrix.

**Keywords:** oxy-fuel combustion; NO<sub>x</sub> reduction; pyridinic nitrogen; pyrrolic nitrogen; synthetic coal; mineral effect

## 1. Introduction

Coal combustion in utility power plants is one of the largest contributors to the anthropogenic emission of carbon dioxide (CO<sub>2</sub>), which also brings about many environmental pollution problems, such as nitrogen oxides (NO<sub>x</sub>), sulfur oxides (SO<sub>x</sub>), particulate matters (PMs), mercury (Hg), and so on [1–7]. Several approaches can be utilized to reduce CO<sub>2</sub> emissions originating from coal-fired power plants, including the improvement of thermal efficiency, the replacement of coal with low-carbon fuels, the introduction of combined cycles, and the capture and storage of CO<sub>2</sub> (CCS) [8–12]. Oxy-fuel combustion can not only capture CO<sub>2</sub> in the large-scale but also obviously lower NO<sub>x</sub> emission in coal-fired power plants [13–20], which is a potential clean coal technology in the near future and is drawing an ever-increasing attention nowadays.

Numerous studies have been carried out on NO<sub>x</sub> emission in oxy-fuel combustion using various coals from different regions [21–26]. Ndibe et al. [22] indicated that compared to the air condition, nitric oxide (NO) emission was reduced obviously during oxy-fuel combustion, while the presence of steam could further lower the formation of NO from coal nitrogen and diminish the recycled NO. Ikeda et al. [27] believed that the NO<sub>x</sub> emission per unit of energy in oxy-fuel combustion was nearly

70% lower than that in the air case. Notwithstanding, Lupianez et al. [28] reported close emissions of  $\text{NO}_x$  per energy unit between the air and oxy-fuel conditions using a bubbling fluidized bed combustor, while Lasek et al. [29] found out that the NO content in oxy-fuel combustion was less than one-third in air using a pressurized fluidized bed combustor. Under the oxy-fuel condition with gas recirculation, the emission of NO per energy unit could be reduced by 70–75% compared to air combustion from experiments performed by Andersson et al. [30]. However, Alves et al. [31] pointed out that the conversion rates of  $\text{NH}_3$ -to- $\text{NO}_x$  in the air and a 20.9%  $\text{O}_2$ /79.1%  $\text{CO}_2$  atmosphere showed similarity, but the increase of  $\text{O}_2$  concentration had an obvious promotion on NO formation. The  $\text{NO}_x$  emission in  $\text{O}_2$ / $\text{CO}_2$  atmosphere was roughly 20% lower than that in the air, while the  $\text{NO}_x$  emission under the condition with recycled flue gas was considerably reduced by approximately 50% [27]. Conclusions drawn by different investigators were still inconsistent possibly due to the complexity and differences of coal samples.

The previous research showed that the influences of combustion temperature on NO formation from volatile-N were contrary between reducing and oxidizing atmospheres [32]. The increase in pressure did not significantly affect the NO creation but generated preferential conditions for NO reduction [29]. Stadler et al. [21] believed that the flue gas recirculation could result in a reduction of  $\text{NO}_x$  emission by 40–50%, and that wet recycling was preferable in term of  $\text{NO}_x$  reduction due to the inhibition effect of  $\text{H}_2\text{O}$  on the oxidation of intermediates to form NO. Shaddix and Molina [33] concluded that NO reburn fraction was between 20% and 40% in oxy-fuel combustion. The stream staging was more efficient for the reduction of  $\text{NO}_x$  in oxy-CFB combustion than that in air staging from experiments conducted by Duan et al. [34]. The little formation of thermal- $\text{NO}_x$ , the destruction of recycled  $\text{NO}_x$ , and the reduction of  $\text{NO}_x$  on char surfaces by the high concentration of local carbon monoxide (CO) all have contributions to the reduction of  $\text{NO}_x$  during oxy-fuel combustion. Sometimes, experimental results from various researchers could differ significantly from one another due to the inherent complexity of coal compositions. In addition, compared to air combustion, the influence of inherent minerals on  $\text{NO}_x$  reduction in oxy-fuel combustion still remains poorly understood. The direct utilization of coal is difficult for exploring the effects of specific minerals on  $\text{NO}_x$  formation and sometimes it is almost impossible to avoid the complicated interactions from other minerals. Few investigators have aimed at the combustion atmosphere dependence of mineral effect on  $\text{NO}_x$  reduction. Little work, if any, has been carried out on the impacts of oxy-fuel combustion on the transformation of different nitrogen functional groups. The evolutions of NO and nitrogen dioxide ( $\text{NO}_2$ ) formation with coal particle size are still unclear under oxy-fuel condition. Some scholars believed that the enlargement of coal particle size lowered the devolatilization rate but had a slight impact on char-nitrogen in the air, while others found out that the release of char-nitrogen presented an obvious positive correlation with particle size [35]. Conclusions from various scholars are probably different and sometimes are even contradictory.

Synthetic coals can be utilized to further probe  $\text{NO}_x$  formation and reduction for its known and simple compositions. Our previous studies indicated that synthetic coals retained the main structure and property of the aromatic heterocyclic rings, simplified the coal macromolecule, and had definite chemical compositions and nitrogen functional groups [23,36]. In addition, the combustion characteristics of synthetic coal under oxy-fuel conditions present a striking similarity to those of high volatile coal [36]. Hence, the application of synthetic coal can offer an improved understanding of  $\text{NO}_x$  behaviors in oxy-fuel combustion. The complicated catalytic interactions can be avoided and a specific study on the influence of certain mineral matter can be achieved due to the convenient control of mineral matters within the coal matrix. Unfortunately, synthetic coal has not been employed to elucidate the  $\text{NO}_x$  formation and its reduction mechanisms in oxy-fuel combustion yet.

Based on the advantages of synthetic coal for research on the transformation of coal nitrogen, the present objective was to study the  $\text{NO}_x$  reduction in oxy-fuel combustion using two synthetic coals with pyrrolic or pyridinic nitrogen employing a lab-scale entrained flow reactor. The influences of the combustion atmosphere on the fuel nitrogen (denoted as fuel-N, hereafter) transformation of the two

main nitrogen functional groups in the coal matrix were experimentally compared. The impacts of coal particle size on NO and NO<sub>2</sub> formation were also evaluated contrastively. In addition, the effects of mineral matters on NO<sub>x</sub> reduction were elucidated. The present study will provide a supplementary information on the mechanisms of NO<sub>x</sub> formation and reduction in oxy-fuel combustion.

## 2. Materials and Methods

### 2.1. Sample Preparation

Two synthetic coals with a specific kind of nitrogen functional group (also known as fuel nitrogen) were prepared from nitrogen compounds and cellulose by compaction heat-treatment using an electrical-heating high-pressure reactor, as illustrated in Figure 1. Here, two nitrogen compounds, 8-hydroxyquinoline (C<sub>9</sub>H<sub>7</sub>NO) and 4-hydroxycarbazole (C<sub>12</sub>H<sub>9</sub>NO), were used to synthesize synthetic coals with cellulose according to our previous work [36]. The synthetic coals have physical properties highly similar to real coals. The X-ray photoelectron spectroscopic (XPS) analysis demonstrated that only one binding energy peak appears at 398.4 eV or 400.7 eV in two synthetic coals as illustrated in Figure 2, indicating fuel nitrogen of pyridinic or pyrrolic forms in two synthetic coals, respectively. The compaction heat-treatment did not change the chemical form of fuel nitrogen from 8-hydroxyquinoline or 4-hydroxycarbazole. The synthetic coal with pyridinic nitrogen was denoted as “M6” hereafter, while the other containing pyrrolic nitrogen was denoted as “M5”.

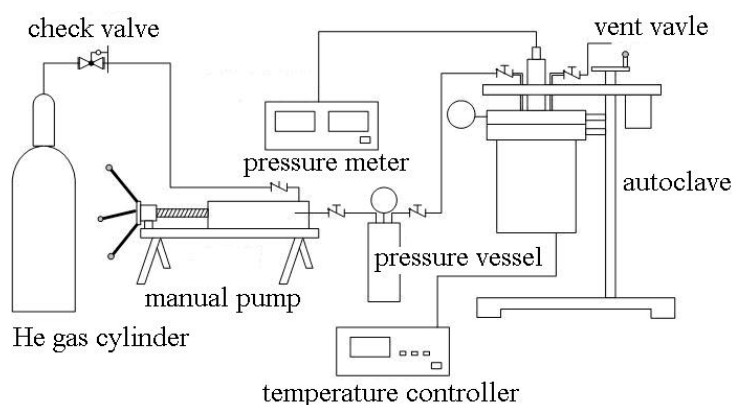


**Figure 1.** The schematic diagram of the experimental system for synthesizing coal samples.

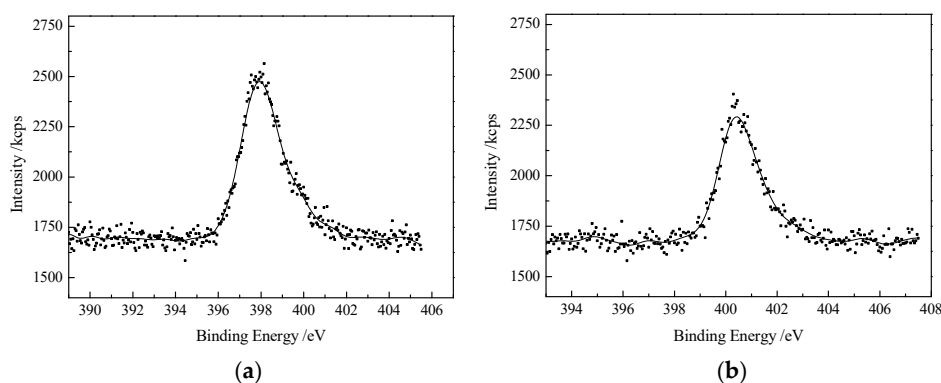


**Figure 2.** The binding energy curves of fuel nitrogen in synthetic coal samples. (a) Synthetic coal “M6”; (b) Synthetic coal “M5”.

Two real coals were chosen for comparison including Qiancheng bituminous coal (QC) and Pingzhuang lignite (PZ). The proximate and ultimate analyses of experimental fuel samples are listed in Table 1. No ash nor sulphur was present in synthetic coals due to the absence of corresponding constituents in the preparation materials. The reactivity of synthetic coal demonstrated a close

resemblance to that of lignite during oxy-fuel combustion [36]. Hence, the synthetic coal is a highly effective substitute for coals in term of in-depth research on the transformation of fuel nitrogen and  $\text{NO}_x$  reduction under oxy-fuel conditions. Three mineral matters, ferric oxide ( $\text{Fe}_2\text{O}_3$ ), sodium carbonate ( $\text{Na}_2\text{CO}_3$ ), and calcium carbonate ( $\text{CaCO}_3$ ), were used to investigate the catalytic effects of minerals on the formation and reduction of  $\text{NO}_x$  from different functional groups of fuel nitrogen. Each additive of 5% by weight was loaded with synthetic coals during the present experiments.

**Table 1.** The proximate and ultimate analyses of real and synthetic coals (wt%, d).

Coal Code	BET $\text{m}^2 \text{g}^{-1}$	Fuel Ratio ( $w(\text{FC})/w(\text{V})$ )	Proximate Analysis				Ultimate Analysis			
			$w(\text{FC})$	$w(\text{V})$	$w(\text{A})$	$w(\text{C})$	$w(\text{H})$	$w(\text{O})^a$	$w(\text{N})$	$w(\text{S})$
QC	3.87	2.5	46.31	18.26	35.43	55.36	3.12	4.64	1.10	0.35
PZ	9.37	1.2	38.77	31.22	30.01	50.58	3.42	14.09	0.90	1.00
M6	4.12	2.2	68.90	31.10	0.00	65.39	2.86	28.30	3.45	0.00
M5	4.31	2.2	68.47	31.53	0.00	68.12	3.09	25.96	2.83	0.00

<sup>a</sup> calculated by the subtraction method in the percentage of weight.

## 2.2. Experimental Setup

A lab-scale entrained flow reactor was employed to investigate the  $\text{NO}_x$  conversion during the oxy-fuel combustion of synthetic coals as shown in Figure 3, which can realize the rapid combustion of fine coal particles with a preset stable feeding rate. The experimental reactor had an inside diameter of 32 mm and was heated by an electrical heating furnace. The temperature was monitored by an S-type thermocouple. Before the rapid combustion experiments, the reactor was heated to a preset temperature, a sample of 0.1 g was loaded in the micro-feeder in advance, and the system was purged by the desired gas mixture at room temperature. The total flow rate of the mixture gas was  $1000 \text{ mL}\cdot\text{min}^{-1}$ , while the whole gas mixture was split into two streams. The primary (oxidizer carrying the solid fuel) flow rate was  $200 \text{ mL}\cdot\text{min}^{-1}$  and used to entrain the sample into the reactor with a feeding rate of  $0.04 \text{ g}\cdot\text{min}^{-1}$ . The oxygen concentration in experiments of oxy-fuel combustion ranged from 10% to 50%. The outlet concentrations of gas species were continuously analyzed by an FTIR gas analyzer Gasmeter DX-4000. All experiments were carried out at least three times for repeatability and the results were averaged. Here, a micro-feeder was specially designed to ensure the micro-scale, continuous, and stable feeding of fine solid particles as the enlarged insect depicted in Figure 3. The feeding rate can be adjusted by the flow rate of the stream and the rotation speed of the stepping motor.

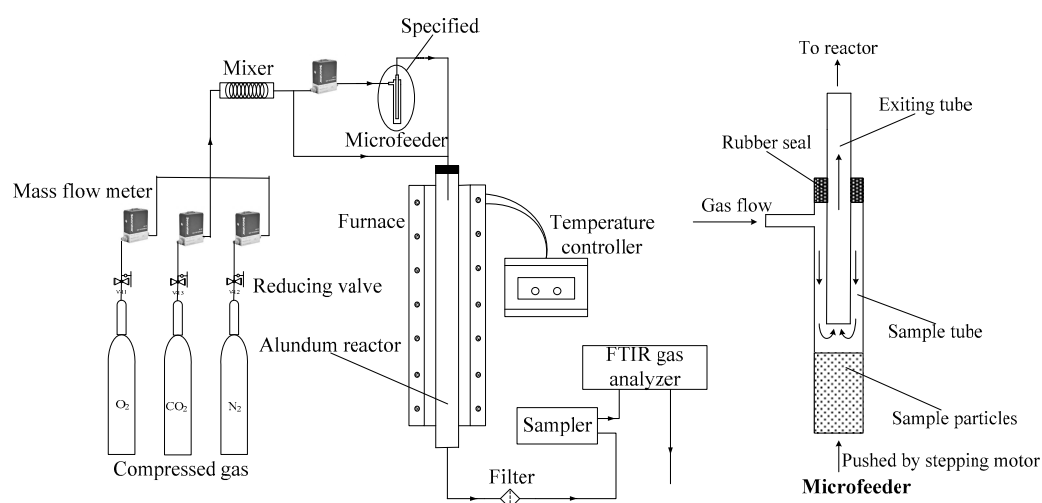


**Figure 3.** The schematic diagram of the experimental system for  $\text{NO}_x$  emission during air and oxy-fuel combustion.

Due to the content differences of fuel nitrogen in various samples, the comparison between the amounts of nitrogen species cannot reasonably demonstrate the transformation behaviors of various nitrogen functional groups. Here, the conversion ratios of fuel-nitrogen to nitrogen oxides (NO, N<sub>2</sub>O, and NO<sub>2</sub>) were employed to investigate the transformation of fuel nitrogen during air and oxy-fuel combustion. The emission content of nitrogen oxides was calculated from the integral of nitrogen oxide concentration within the duration of a certain time.  $X_{\text{NO}}$ ,  $X_{\text{N}_2\text{O}}$ , and  $X_{\text{NO}_2}$  (%) were used to represent the conversion ratios of fuel-nitrogen to NO, N<sub>2</sub>O, and NO<sub>2</sub> during combustion within  $\Delta t$ , calculated as follows:

$$X_{\text{NO-N}} = \frac{\int_{t_0}^{t_0+\Delta t} F \cdot C_{\text{NO}} \cdot 10^{-6} \cdot dt / 22.4}{M \cdot N_d / 14} \times 100 \quad (1)$$

$$X_{\text{N}_2\text{O-N}} = \frac{\int_{t_0}^{t_0+\Delta t} F \cdot C_{\text{N}_2\text{O}} \cdot 10^{-6} \cdot dt / 22.4}{M \cdot N_d / 14} \times 100 \quad (2)$$

$$X_{\text{NO}_2\text{-N}} = \frac{\int_{t_0}^{t_0+\Delta t} F \cdot C_{\text{NO}_2} \cdot 10^{-6} \cdot dt / 22.4}{M \cdot N_d / 14} \times 100 \quad (3)$$

where  $F$  is the volumetric flow, L·s<sup>-1</sup>;  $M$  is the sample weight, g;  $t_0$  is the time at which the measurement begins, s;  $\Delta t$  is the measurement duration, s;  $N_d$  is the nitrogen content in the sample, %;  $C_{\text{NO}}$ ,  $C_{\text{N}_2\text{O}}$ , and  $C_{\text{NO}_2}$  are the concentrations of NO, N<sub>2</sub>O, and NO<sub>2</sub> in flue gas, respectively,  $\mu\text{L}\cdot\text{L}^{-1}$ . The volume of each mole ideal gas is 22.4 L at the standard condition ( $t = 273.15 \text{ K}$ ,  $p = 101325 \text{ Pa}$ ), while the atomic weight of nitrogen is 14.

### 3. Results

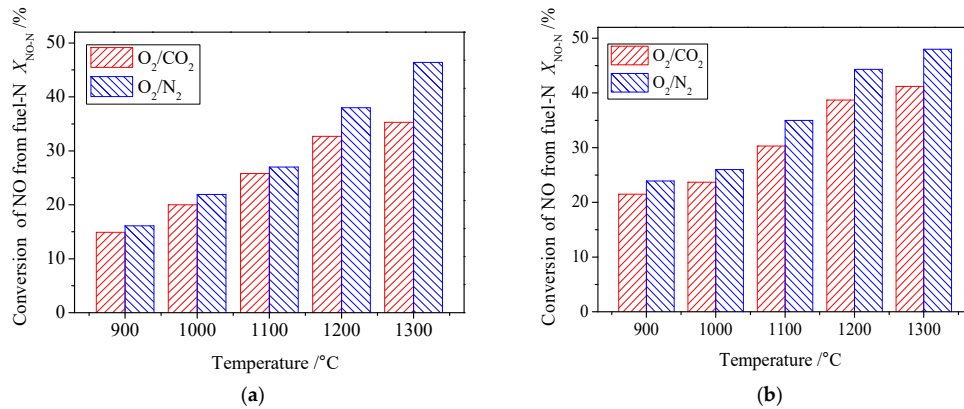
#### 3.1. Influence of Combustion Atmosphere on the Oxidation of Different Nitrogen Functional Groups

The change of the combustion atmosphere presents a certain influence on the transformation of coal nitrogen. NO accounts for a predominant fraction of NO<sub>x</sub> during the combustion of pulverized coal. Therefore, NO was extensively focused on in existing research. Figure 4 illustrates the comparisons of NO conversion from variation fuel nitrogen between oxy-fuel and air combustion with a particle size of 63–98  $\mu\text{m}$ . Regardless of the chemical form of fuel nitrogen in synthetic coal, oxy-fuel combustion leads to a certain reduction of NO relative to air condition. Most previous pilot-scale experiments indicated that compared to air combustion, the NO emission in oxy-fuel combustion could be approximately diminished by one-third to two-thirds [21,27,29,30,37], while the extent of NO decline here is only 7–24% dependent on the combustion temperature and the nitrogen functional group. Ikeda et al. [27] observed that the NO<sub>x</sub> emissions in O<sub>2</sub>/CO<sub>2</sub> mixture were decreased by about 20% compared to those in the air, which supports the present result. In the present study, the O<sub>2</sub>/CO<sub>2</sub> mixture stream was purged and mixed from the compressed gas cylinders without flue gas recirculation (FGR), while the FGR was usually regarded as the principal contribution to NO reduction in oxy-fuel combustion due to both the reduction of recirculated NO<sub>x</sub> and the inhibition of fuel-N to NO [21,27,30]. From another aspect, the gas flow under the present experiments was in excess and the oxidizing environment was around the sample particles. Thus, a smaller decline of NO emission was observed due to the fewer reduction reactions associated with NO.

The differences of NO conversion between two atmospheres are increased with the increasing combustion temperature. A higher temperature in oxy-fuel combustion gives rise to more effective reduction impact on NO<sub>x</sub> emission. The elevated content of CO on char surfaces due to the intensified char-CO<sub>2</sub> gasification generates an ever-increasing contribution to NO<sub>x</sub> reduction at high temperature. In addition, the amount of thermal NO<sub>x</sub> in air combustion rises substantially with the combustion temperature while much less thermal NO<sub>x</sub> is formed in oxy-fuel combustion. The conversion to NO from synthetic coal “M5” is higher than that from “M6” at a given temperature. Previous studies indicated that the NO conversion ratios from fuel nitrogen decreased with an increase in nitrogen



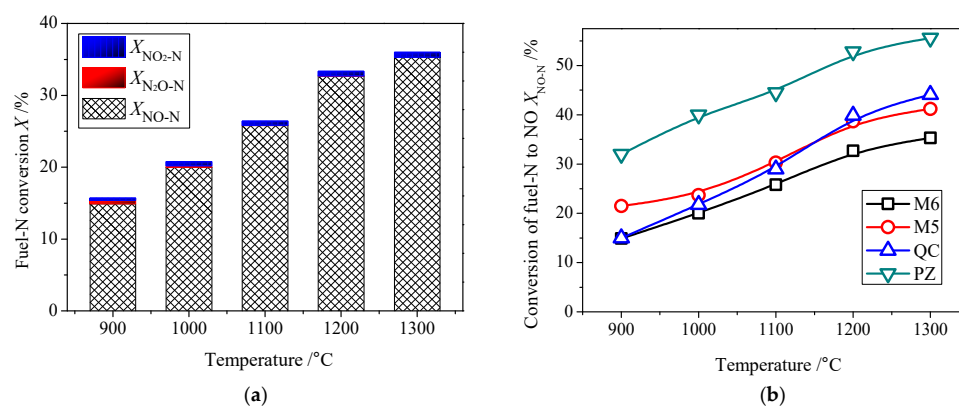
content (dry and ash-free basis) in various coals [38,39], while the conversion of fuel-N to NO show a positive relationship with fuel ratio ( $FC/V$ ) in the present research. Compared with pyridinic nitrogen in coal, more of the pyrrolic nitrogen is converted to NO. Furthermore, an oxy-fuel combustion with  $O_2$  content of 21% exhibits a more effective impact on the reduction of  $NO_2$  than that of NO.



**Figure 4.** The oxidation of different nitrogen functional groups with a combustion atmosphere (21%  $O_2$ ). (a) Synthetic coal "M6"; (b) Synthetic coal "M5".

### 3.2. The Effect of Combustion Temperature on the Formation of $NO_x$

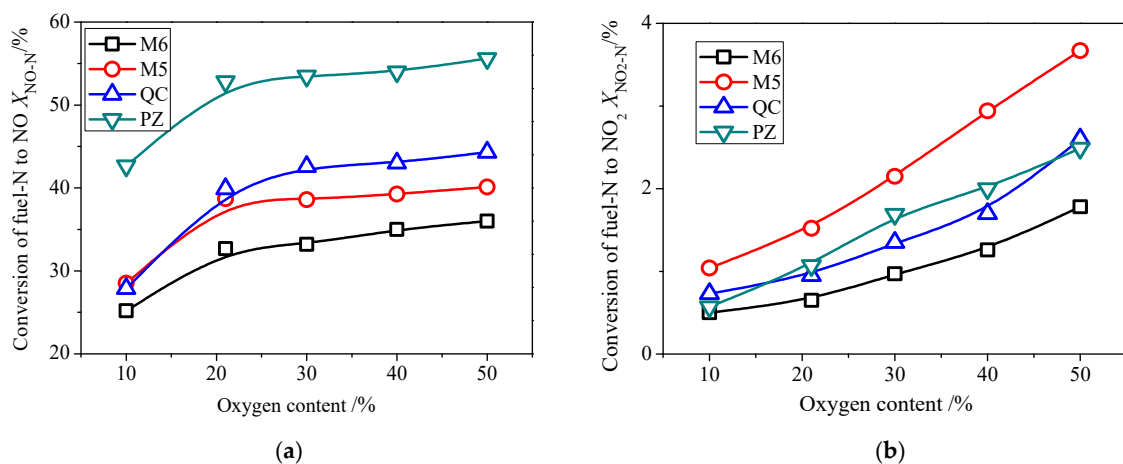
Figure 5 depicts the effect of combustion temperature on the release characteristics of nitrogen species during the rapid oxy-fuel combustion of real and synthetic coals with a particle size of 63–98  $\mu m$  and an  $O_2$  content of 21%. The principal nitrogen species during the present oxy-fuel combustion of synthetic coals is NO with a small amount of  $NO_2$  and  $N_2O$  under certain conditions, similar to the air case. The conversion of NO from fuel-N with the combustion temperature presents striking similarities between synthetic and real coals. The NO emissions in the present experiments are increased obviously with the combustion temperature during the rapid entrained flow combustion, which is consistent with the results obtained by Sun et al. [32] However, Lasek et al. [29] observed that the NO emission increased with the temperature to about 850 °C but the further rise of temperature brought about a decline of the NO formation during the oxy-fuel combustion in a fluidized bed reactor. The formation of  $NO_x$  is largely dependent on the experimental conditions. Moreover, the competition between conversions of fuel-N to NO and char-NO reactions occurs on char surfaces with the combustion temperature. The emission of  $NO_2$  is also increased slightly with temperature while none  $N_2O$  is generated above 1000 °C. With the evolution of the combustion temperature, the conversions of fuel-N to NO from synthetic coal "M6" exhibits a synchronous variation tendency with those of "M5", while the conversion ratios vary with a difference of about five percentage points. The oxidation ratios of the different fuel nitrogen values varied at a given identical condition.



**Figure 5.** The effect of temperature on the release behaviors of nitrogen species under the 21%  $O_2$ /79%  $CO_2$  condition. (a) Nitrogen oxides from "M6"; (b) NO release behaviors.

### 3.3. Comparison of the NO and NO<sub>2</sub> Emissions with Oxygen Content

The oxygen content in oxy-fuel combustion can be regulated by adjusting the ratio and location of FGR while it also yields an impact on the coal reactivity and NO<sub>x</sub> emission. The effects of oxygen content on NO<sub>x</sub> emissions at the combustion temperature of 1200 °C are illustrated in Figure 6. The NO conversion increases with the oxygen content, as shown in Figure 6a. The effect of oxygen variation on the NO emission is significant as the O<sub>2</sub> content is below 21%, while the increase extent of NO conversion is slowed down with an O<sub>2</sub> content beyond 21%. Ndibe et al. [22] and Duan et al. [34] also observed an increase in NO emission with oxygen concentration for the cases of oxy-fuel combustion, while Shaddix and Molina [33] concluded that the conversion of fuel-nitrogen to NO<sub>x</sub> increased notably with the oxygen content, which is similar to the present study. The oxidation reactions of fuel-N are promoted by increasing oxygen content. More oxygen leads to less CO on char surfaces and the oxidizing atmosphere around the char particles impedes the NO reduction. As for the principal NO<sub>x</sub> precursor, NH<sub>3</sub>, the conversion rate of NH<sub>3</sub>-to-NO<sub>x</sub> can be increased obviously with the raised O<sub>2</sub> concentration under oxy-fuel conditions [31]. Whereas, the further access of oxygen content cannot considerably enlarge the NO conversion, which is beneficial for the NO<sub>x</sub> reduction during oxy-fuel combustion. Zhao et al. [40] investigated the oxidation of pyridine at 1000 °C and indicated that the NO conversion cannot continue to increase with the oxygen content, which is consistent with the present experimental result of synthetic coal with pyridinic nitrogen.



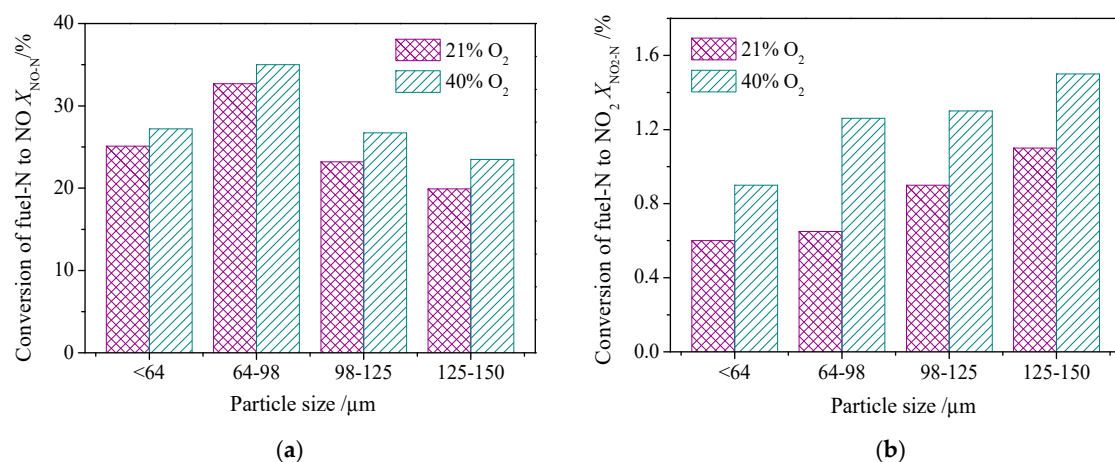
**Figure 6.** The comparison between NO and NO<sub>2</sub> emissions with oxygen content at 1200 °C under the oxy-fuel condition. (a) Conversion to NO; (b) Conversion to NO<sub>2</sub>.

Figure 6b shows the evolution of NO<sub>2</sub> conversion ratio with the oxygen content. The variation of NO<sub>2</sub> conversion is roughly proportional to oxygen content, largely different from the case of NO. The NO<sub>2</sub>/NO<sub>x</sub> ratios present a slightly increasing tendency with the oxygen content in oxy-fuel combustion, which is in accordance with results obtained by Ndibe et al. [22]. The access O<sub>2</sub> can further enhance the conversion of NO to NO<sub>2</sub>, which also has a certain association with the slow-down increase of NO. The rise in the concentration of oxidizing radicals from high oxygen inlet content is responsible for the promotion of NO<sub>2</sub> formation as well. The rise of O<sub>2</sub> content not only promotes the formation of NO, but also intensifies the further oxidation of already-formed NO to NO<sub>2</sub>. Consequently, compared with NO, the increase of the oxygen partial pressure in the oxidant has a more obvious promotion effect with respect to the NO<sub>2</sub> formation. It can be seen from Figure 6b that, the conversions of NO<sub>2</sub> from synthetic coal “M5” are considerably higher than those from “M6”. Fuel nitrogen of pyrrolic form is inclined to transform into NO<sub>2</sub> under the condition of a high O<sub>2</sub> content in oxy-fuel combustion. The NO conversion from PZ lignite is the highest while the case of NO<sub>2</sub> is different. The conversion of NO<sub>x</sub> (sum of NO and NO<sub>2</sub>) from fuel nitrogen is reduced with an increase in the nitrogen content of dry ash-free basis within coal matrix. Coal with a high level of pyrrolic nitrogen

favors the formation of NO<sub>2</sub> compared with others. Hence, the coal property and chemical form of fuel nitrogen exhibit distinct influences on the formation and destruction of NO<sub>x</sub> during the oxy-fuel combustion of coal-based fuels.

### 3.4. Particle Size Dependence of NO and NO<sub>2</sub> Emission

The influences of coal particle size on transformation behaviors of fuel nitrogen in coal are still ambiguous, especially the possibly different particle size dependence of NO and NO<sub>2</sub>. Figure 7 illustrates the effect of particle size on the NO<sub>x</sub> release from synthetic coal “M6” with pyridinic nitrogen under the oxy-fuel condition of 1200 °C. It can be observed from Figure 7a that with the increase of particle size, the conversion ratio of NO from fuel nitrogen first increases and then decreases with the maximum conversion ratio present at a particle size of 64–98 μm. This can be explained by the competition between char-O<sub>2</sub> reactions and char-NO reactions on particle surfaces. On surfaces of larger particles, the char-O<sub>2</sub> reactions are further enhanced which gives rise to a decrease in NO formation [29]. The particle size dependence of the NO<sub>2</sub> conversion ratio from fuel nitrogen of pyridinic form differs greatly from the case of NO. As depicted in Figure 7b, the NO<sub>2</sub> conversion is increased with the particle size in the range of <150 μm. The transformation of nitrogen-containing functional groups in coal is strongly affected by the specific surface area of the coal particles. Compared with “M6”, the synthetic coal “M5” shows a similar relationship between particle size and NO<sub>x</sub> emission.



**Figure 7.** The particle size dependence of NO and NO<sub>2</sub> emissions at 1200 °C under the oxy-fuel condition. (a) Conversion to NO; (b) Conversion to NO<sub>2</sub>.

### 3.5. Mineral Impacts on the Transformation of Fuel Nitrogen

The ash and sulfur were absent in synthetic coals on account of the none corresponding constituents in raw materials, which is beneficial to probe the influence of certain mineral matters on NO<sub>x</sub> reduction during oxy-fuel combustion compared with air. Figure 8 shows the effects of Fe<sub>2</sub>O<sub>3</sub>, Na<sub>2</sub>CO<sub>3</sub>, and CaCO<sub>3</sub> on NO<sub>x</sub> emission during air and oxy-fuel combustion. The mineral matters establish the same influence tendency on NO conversion from pyridinic nitrogen of synthetic coal between O<sub>2</sub>/CO<sub>2</sub> and O<sub>2</sub>/N<sub>2</sub> atmospheres as shown in Figure 8a,b. The catalytic effects of sodium (Na), calcium (Ca), and iron (Fe) on the oxidation of pyridinic nitrogen are independent of the combustion atmosphere, and the change from air to oxy-fuel combustion has a negligible relevance to the impacts of mineral addition on the transformation behaviors of pyridinic nitrogen. When the combustion temperature is 1000 °C, the additive Fe<sub>2</sub>O<sub>3</sub> reduces the NO conversion while Na<sub>2</sub>CO<sub>3</sub> and CaCO<sub>3</sub> can promote the formation of NO. The presence of Fe<sub>2</sub>O<sub>3</sub> possibly promotes the reduction of NO to N<sub>2</sub> via the following reactions [41,42]:





The conversion of NO from synthetic coal with pyridinic nitrogen has the following sequence:  $\text{Na}_2\text{CO}_3 > \text{CaCO}_3 > \text{without-mineral} > \text{Fe}_2\text{O}_3$ . However, the addition of these minerals all reduces the NO emission at 1200 °C with the following sequence of NO conversion from pyridinic nitrogen: without-mineral  $> \text{Na}_2\text{CO}_3 > \text{CaCO}_3 > \text{Fe}_2\text{O}_3$ . The contribution of minerals on the transformation of fuel nitrogen is strongly affected by two competitive aspects during oxy-fuel combustion: the catalytic effect on oxidation of fuel nitrogen and the impact on the heterogeneous reduction of  $\text{NO}_x$  on char surfaces.

As Figure 8c,d depicted that the influence of mineral matter on the oxidation of pyrrolic nitrogen differs significantly from the case of pyridinic nitrogen. Only the addition of  $\text{Fe}_2\text{O}_3$  leads to a decline of NO conversion from pyrrolic nitrogen, while both  $\text{Na}_2\text{CO}_3$  and  $\text{CaCO}_3$  facilitate the release of NO. Moreover, the mineral matters generate different influences on the oxidation of pyridinic nitrogen under  $\text{O}_2/\text{CO}_2$  and  $\text{O}_2/\text{N}_2$  conditions. The conversion of NO from a synthetic coal sample with  $\text{Na}_2\text{CO}_3$  additive exceeds that with  $\text{CaCO}_3$  in  $\text{O}_2/\text{CO}_2$  atmosphere at 1000 °C, which differs from the air case. Compared with air circumstance, oxy-fuel combustion causes the change of the mineral catalytic effect on the transformation of pyrrolic nitrogen within the organic structure of coal. The combustion temperature and species of mineral matters exhibit various influences on the formation and reduction of  $\text{NO}_x$  during the oxy-fuel combustion of coals.

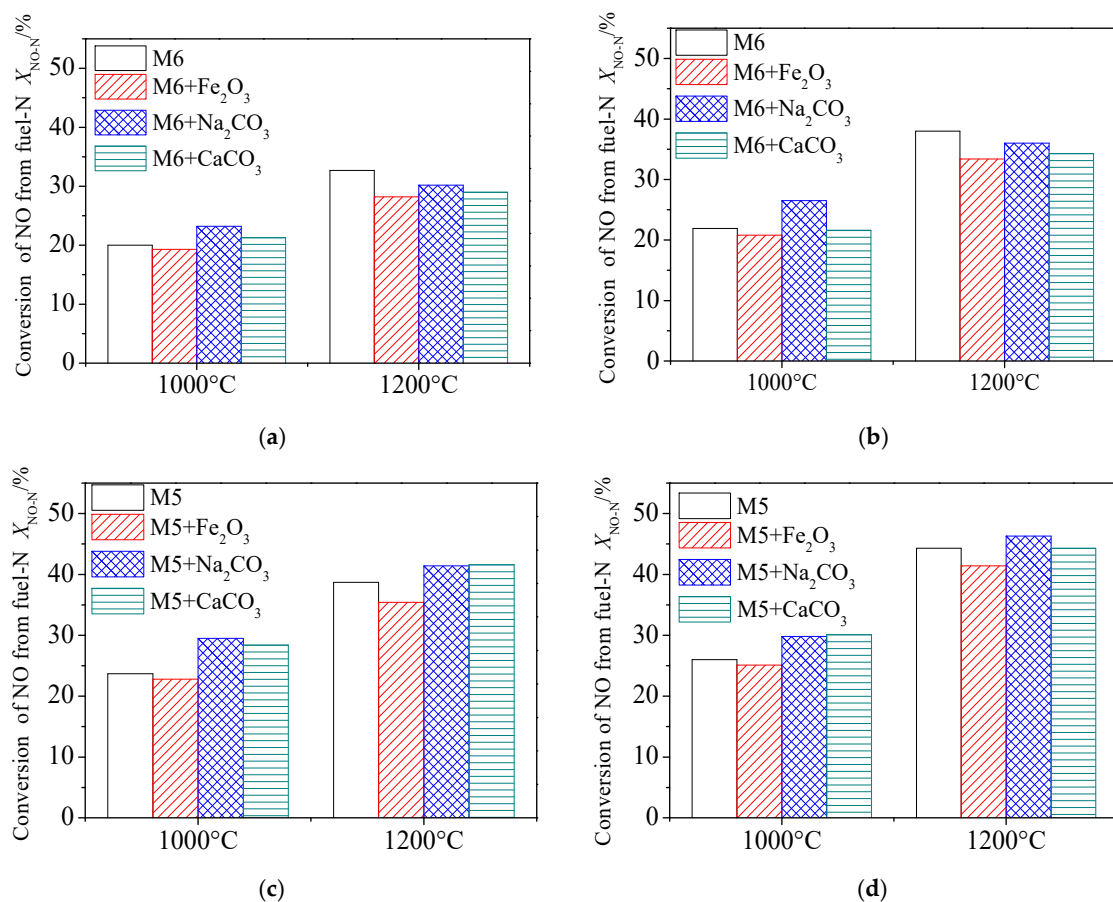


**Figure 8.** The effects of mineral matters on  $\text{NO}_x$  emission during air and oxy-fuel combustion. (a) "M6" in 21%  $\text{O}_2/79\%$   $\text{CO}_2$  atmosphere; (b) "M6" in 21%  $\text{O}_2/79\%$   $\text{N}_2$  atmosphere; (c) "M5" in 21%  $\text{O}_2/79\%$   $\text{CO}_2$  atmosphere; (d) "M5" in 21%  $\text{O}_2/79\%$   $\text{N}_2$  atmosphere.

#### 4. Conclusions

The formation and reduction of  $\text{NO}_x$  in oxy-fuel combustion were experimentally investigated in a lab-scale entrained flow reactor using two synthetic coals with pyrrolic or pyridinic nitrogen.

The oxidation process of fuel nitrogen in synthetic coal presented a striking similarity to that in real coal. The differences of NO conversion from fuel nitrogen between the oxy-fuel and air conditions were enlarged with the combustion temperature. The pyrrolic nitrogen was more inclined to be oxidized into NO<sub>x</sub> compared with pyridinic nitrogen. The NO emission first increased significantly and then trended to an asymptotic constant with the O<sub>2</sub> content elevated between 10–50%. Whereas the variation of NO<sub>2</sub> conversion was roughly proportional to the oxygen content, and this was distinctly different from the condition of NO. The particle size dependence of NO<sub>2</sub> conversion from pyridinic nitrogen was greatly unlike the case of NO. The conversion of NO<sub>2</sub> from fuel nitrogen increased with the particle size, while the formation of NO showed a non-monotonic variation. The catalytic effects of sodium, calcium, and iron on the oxidation of pyridinic nitrogen were independent of combustion atmosphere, but the oxy-fuel combustion gave rise to a change of the mineral catalytic effect on the transformation of pyrrolic nitrogen compared with air combustion. In addition, the kinds of mineral matter indeed generated different influences on the oxidation of various nitrogen functional groups.

**Author Contributions:** Conceptualization, C.W.; Methodology, P.W. and L.Z.; Validation, C.W., and Y.D.; Formal analysis, C.W. and Y.D.; Investigation, P.W., L.Z., and Y.D.; Writing—original draft preparation, C.W.; Writing—review and editing, C.W. and D.C.; Supervision, D.C.; Project administration, C.W.; Funding acquisition, C.W.

**Funding:** This research was funded by the National Key R&D Program of China, grant number 2017YFB0602003.

**Acknowledgments:** The authors acknowledge financial support from the National Key R&D Program of China (2017YFB0602003).

**Conflicts of Interest:** The authors declare no conflict of interest.

## References

1. Xin, H.H.; Wang, D.M.; Qi, X.Y.; Qi, G.S.; Dou, G.L. Structural characteristics of coal functional groups using quantum chemistry for quantification of infrared spectra. *Fuel Process. Technol.* **2014**, *118*, 287–295. [[CrossRef](#)]
2. Xin, H.H.; Wang, D.M.; Qi, X.Y.; Zhong, X.X.; Ma, L.Y.; Dou, G.L.; Wang, H.T. Oxygen consumption and chemisorption in low-temperature oxidation of sub-bituminous pulverized coal. *Spectrosc. Lett.* **2018**, *51*, 104–111. [[CrossRef](#)]
3. Jayaraman, K.; Kok, M.V.; Gokalp, I. Pyrolysis, combustion and gasification studies of different sized coal particles using TGA-MS. *Appl. Therm. Eng.* **2017**, *125*, 1446–1455. [[CrossRef](#)]
4. Jayaraman, K.; Kok, M.V.; Gokalp, I. Thermogravimetric and mass spectrometric (TG-MS) analysis and kinetics of coal-biomass blends. *Renew. Energy* **2017**, *101*, 293–300. [[CrossRef](#)]
5. Mathews, J.P.; Miller, B.G.; Song, C.S.; Schobert, H.H.; Botha, F.; Finkleman, R.B. The EBB and flow of US coal research 1970-2010 with a focus on academic institutions. *Fuel* **2013**, *105*, 1–12. [[CrossRef](#)]
6. Suresh, M.; Reddy, K.S.; Kolar, A.K. Thermodynamic analysis of a coal-fired power plant repowered with pressurized pulverized coal combustion. *Proc. Inst. Mech. Eng. Part A* **2012**, *226*, 5–16. [[CrossRef](#)]
7. Elfeky, A.Y.; Abdelkhalek, M.F.; Kamal, M.M. Pulverized coal combustion with opposing/cross-flow methane/air mixtures. *Proc. Inst. Mech. Eng. Part A* **2014**, *228*, 688–707. [[CrossRef](#)]
8. Kok, M.V. Carbon capture and storage: Current perspectives, re-use activities, and future prospects in Turkey. *Energy Sources Part A* **2015**, *37*, 1979–1987. [[CrossRef](#)]
9. Li, W.; Li, S.Y.; Xu, M.X.; Wang, X. Study on the limestone sulfation behavior under oxy-fuel circulating fluidized bed combustion condition. *J. Energy Inst.* **2018**, *91*, 358–368. [[CrossRef](#)]
10. Li, W.; Xu, M.X.; Li, S.Y. Calcium sulfation characteristics at high oxygen concentration in a 1MW(th) pilot scale oxy-fuel circulating fluidized bed. *Fuel Process. Technol.* **2018**, *171*, 192–197. [[CrossRef](#)]
11. Mansouri, M.T.; Mousavian, S.M. Exergy-based analysis of conventional coal-fired power plant retrofitted with oxy-fuel and post-combustion CO<sub>2</sub> capture systems. *Proc. Inst. Mech. Eng. Part A* **2012**, *226*, 989–1002. [[CrossRef](#)]
12. Jayanti, S.; Saravanan, V.; Sivaji, S. Assessment of retrofitting possibility of an Indian pulverized coal boiler for operation with Indian coals in oxy-coal combustion mode with CO<sub>2</sub> sequestration. *Proc. Inst. Mech. Eng. Part A* **2012**, *226*, 1003–1013. [[CrossRef](#)]

13. Wall, T.; Liu, Y.; Spero, C.; Elliott, L.; Khare, S.; Rathnam, R.; Zeenathal, F.; Moghtaderi, B.; Buhre, B.; Sheng, C.; et al. An overview on oxyfuel coal combustion—State of the art research and technology development. *Chem. Eng. Res. Des.* **2009**, *87*, 1003–1016. [[CrossRef](#)]
14. Toftegaard, M.B.; Brix, J.; Jensen, P.A.; Glarborg, P.; Jensen, A.D. Oxy-fuel combustion of solid fuels. *Prog. Energy Combust. Sci.* **2010**, *36*, 581–625. [[CrossRef](#)]
15. Chen, L.; Yong, S.Z.; Ghoniem, A.F. Oxy-fuel combustion of pulverized coal: Characterization, fundamentals, stabilization and CFD modeling. *Prog. Energy Combust. Sci.* **2012**, *38*, 156–214. [[CrossRef](#)]
16. Stanger, R.; Wall, T.; Spoerl, R.; Paneru, M.; Grathwohl, S.; Weidmann, M.; Schefflmecht, G.; McDonald, D.; Myohanen, K.; Ritvanen, J.; et al. Oxyfuel combustion for CO<sub>2</sub> capture in power plants. *Int. J. Greenh. Gas Control* **2015**, *40*, 55–125. [[CrossRef](#)]
17. Ipek, O.; Gurel, B.; Kan, M. Numerical analysis of oxy-coal combustion system burning pulverized coal mixed with different flue gas mass flow rates. *J. Energy Eng.* **2017**, *143*, 04016053. [[CrossRef](#)]
18. Bu, C.S.; Gomez-Barea, A.; Leckner, B.; Chen, X.P.; Pallares, D.; Liu, D.Y.; Lu, P. Oxy-fuel conversion of sub-bituminous coal particles in fluidized bed and pulverized combustors. *Proc. Combust. Inst.* **2017**, *36*, 3331–3339. [[CrossRef](#)]
19. Wang, W.K.; Bu, C.S.; Gomez-Barea, A.; Leckner, B.; Wang, X.Y.; Zhang, J.B.; Piao, G.L. O<sub>2</sub>/CO<sub>2</sub> and O<sub>2</sub>/N<sub>2</sub> combustion of bituminous char particles in a bubbling fluidized bed under simulated combustor conditions. *Chem. Eng. J.* **2018**, *336*, 74–81. [[CrossRef](#)]
20. Mousavian, S.M.; Mansouri, M.T. Conceptual feasibility study of retrofitting coal-fired power plant with oxy-fuel combustion. *Proc. Inst. Mech. Eng. Part A* **2011**, *225*, 689–700. [[CrossRef](#)]
21. Stadler, H.; Christ, D.; Habermehl, M.; Heil, P.; Kellermann, A.; Ohliger, A.; Toporov, D.; Kneer, R. Experimental investigation of NO<sub>x</sub> emissions in oxycoal combustion. *Fuel* **2011**, *90*, 1604–1611. [[CrossRef](#)]
22. Ndibe, C.; Sporl, R.; Maier, J.; Scheffknecht, G. Experimental study of NO and NO<sub>2</sub> formation in a PF oxy-fuel firing system. *Fuel* **2013**, *107*, 749–756. [[CrossRef](#)]
23. Wang, C.; Du, Y.; Che, D. Study on N<sub>2</sub>O reduction with synthetic coal char and high concentration CO during oxy-fuel combustion. *Proc. Combust. Inst.* **2015**, *35*, 2323–2330. [[CrossRef](#)]
24. Lei, M.; Huang, X.Z.; Wang, C.B.; Yan, W.Q.; Wang, S.L. Investigation on SO<sub>2</sub>, NO and NO<sub>2</sub> release characteristics of Datong bituminous coal during pressurized oxy-fuel combustion. *J. Therm. Anal. Calorim.* **2016**, *126*, 1067–1075. [[CrossRef](#)]
25. He, Y.Z.; Zheng, X.C.; Luo, J.H.; Zheng, H.F.; Zou, C.; Luo, G.Q.; Zheng, C.G. Experimental and numerical study of the effects of steam addition on NO formation during methane and ammonia oxy-fuel combustion. *Energy Fuels* **2017**, *31*, 10093–10100. [[CrossRef](#)]
26. Xu, M.X.; Li, S.Y.; Wu, Y.H.; Jia, L.F.; Lu, Q.G. The characteristics of recycled NO reduction over char during oxy-fuel fluidized bed combustion. *Appl. Energy* **2017**, *190*, 553–562. [[CrossRef](#)]
27. Ikeda, M.; Toporov, D.; Christ, D.; Stadler, H.; Forster, M.; Kneer, R. Trends in NO<sub>x</sub> during pulverized fuel oxy-fuel combustion. *Energy Fuels* **2012**, *26*, 3141–3149. [[CrossRef](#)]
28. Lupianez, C.; Guedea, I.; Bolea, I.; Diez, L.I.; Romeo, L.M. Experimental study of SO<sub>2</sub> and NO<sub>x</sub> emissions in fluidized bed oxy-fuel combustion. *Fuel Process. Technol.* **2013**, *106*, 587–594. [[CrossRef](#)]
29. Lasek, J.A.; Glod, K.; Janusz, M.; Kazalski, K.; Zuwala, J. Pressurized oxy-fuel combustion: A study of selected parameters. *Energy Fuels* **2012**, *26*, 6492–6500. [[CrossRef](#)]
30. Andersson, K.; Normann, F.; Johnsson, F.; Leckner, B. NO emission during oxy-fuel combustion of lignite. *Ind. Eng. Chem. Res.* **2008**, *47*, 1835–1845. [[CrossRef](#)]
31. Alves, M.; Rosa, C.; Costa, M. Effect of the oxidizer composition on the CO and NO<sub>x</sub> emissions from a laboratory combustor operating under oxy-fuel conditions. *Energy Fuels* **2013**, *27*, 561–567. [[CrossRef](#)]
32. Sun, S.Z.; Cao, H.L.; Chen, H.; Wang, X.Y.; Qian, J.A.; Wall, T. Experimental study of influence of temperature on fuel-N conversion and recycle NO reduction in oxyfuel combustion. *Proc. Combust. Inst.* **2011**, *33*, 1731–1738. [[CrossRef](#)]
33. Shaddix, C.R.; Molina, A. Fundamental investigation of NO<sub>x</sub> formation during oxy-fuel combustion of pulverized coal. *Proc. Combust. Inst.* **2011**, *33*, 1723–1730. [[CrossRef](#)]
34. Duan, L.B.; Zhao, C.S.; Zhou, W.; Qu, C.R.; Chen, X.P. Effects of operation parameters on NO emission in an oxy-fired CFB combustor. *Fuel Process. Technol.* **2011**, *92*, 379–384. [[CrossRef](#)]
35. Li, C.Z.; Buckley, A.N.; Nelson, P.F. Effects of temperature and molecular mass on the nitrogen functionality of tars produced under high heating rate conditions. *Fuel* **1998**, *77*, 157–164. [[CrossRef](#)]

36. Wang, C.; Du, Y.; Che, D. Reactivities of coals and synthetic model coal under oxy-fuel conditions. *Thermochim. Acta* **2013**, *553*, 8–15. [[CrossRef](#)]
37. Normann, F.; Andersson, K.; Leckner, B.; Johnsson, F. Emission control of nitrogen oxides in the oxy-fuel process. *Prog. Energy Combust. Sci.* **2009**, *35*, 385–397. [[CrossRef](#)]
38. Zhu, Q.; Grant, K.A.; Thomas, K.M. The effect of Fe catalyst on the release of NO during the combustion of anisotropic and isotropic carbons. *Carbon* **1996**, *34*, 523–532. [[CrossRef](#)]
39. Liu, Y.; Che, D. Releases of NO and its precursors from coal combustion in a fixed bed. *Fuel Process. Technol.* **2006**, *87*, 355–362. [[CrossRef](#)]
40. Zhao, K.; Tan, H.; Zhou, Q.; Hui, S.; Xu, T.; Che, D. Experimental investigation on the oxidation rules of pyridine. *J. Combust. Sci. Technol.* **2004**, *10*, 392–395.
41. Hayhurst, A.N.; Ninomiya, Y. Kinetics of the conversion of NO to N<sub>2</sub> during the oxidation of iron particles by NO in a hot fluidised bed. *Chem. Eng. Sci.* **1998**, *53*, 1481–1489. [[CrossRef](#)]
42. Gradoń, B.; Lasek, J. Investigations of the reduction of NO to N<sub>2</sub> by reaction with Fe. *Fuel* **2010**, *89*, 3505–3509. [[CrossRef](#)]



© 2018 by the authors. Licensee MDPI, Basel, Switzerland. This article is an open access article distributed under the terms and conditions of the Creative Commons Attribution (CC BY) license (<http://creativecommons.org/licenses/by/4.0/>).